Decolorization and Detoxification of Triphenylmethane Dyes by isolated endophytic fungus, *Bjerkandera adusta* SWUSI4 under non-nutritive conditions

Tiancong Gao
  Chongqing Key Laboratory of Plant Resource Conservation and Germplasm Innovation, School of Life Sciences
Dan Qin
  Chongqing Key Laboratory of Plant Resource Conservation and Germplasm Innovation, School of Life Sciences
Shihao Zuo
  Chongqing Key Laboratory of Plant Resource Conservation and Germplasm Innovation, School of Life Sciences
Yajun Peng
  Chongqing Key Laboratory of Plant Resource Conservation and Germplasm Innovation, School of Life Sciences
Jieru Xu
  Chongqing Key Laboratory of Plant Resource Conservation and Germplasm Innovation, School of Life Sciences
Baohong Yu
  Chongqing Key Laboratory of Plant Resource Conservation and Germplasm Innovation, School of Life Sciences
Hongchuan Song
  School of Energy and Environment Science, Solar Energy Research Institute
Jinyan Dong (✉ donjyaa@swu.edu.cn)
  Southwest University

Abstract

Biodecolorization by microorganisms is a potential treatment technique of triphenylmethane (TPM) dyes as they seem to be environmentally safe. In the present study, the decolourization and detoxification of cotton blue, crystal violet, malachite green and methyl violet by endophytic fungi from metal-contaminated, *Sinosenecio oldhamianu*, were investigated. Preliminary screening result indicated that SWUSI4, identified as *Bjerkandera adusta*, demonstrated the best decolorization for the four TPM dyes within 14 days. Furthermore, optimization result demonstrated the decolorization rate could reach above 90% at 24h by live cells of isolate SWUSI4 when 4g biomass was added into 100mL dyes solution with the concentration 50mg L^{-1} and shaking conditions. Moreover, decolorization mechanism analysis shows that the decolorization was caused by isolate SWUSI4 that mainly including both absorption of biomass and/or degradation of enzymes. Biosorption of dyes was attributed to binding to hydroxyl, amino, phosphoryl alkane, and ester-lipids groups based on fourier transform infrared (FTIR) analyses. The biodegradation potential of SWUSI4 was further suggested by the change of peaks in the Ultraviolet-visible (UV-vis) spectra and detection of manganese peroxidase and lignin peroxidase activities. Finally, the phytotoxicity test confirmed that TPM dyes toxicity of the treatment after by SWUSI4 was significantly lower than that before treatment. These results indicate that an endophytic SWUSI4 could be used as a potential TPM dyes adsorption and degradation agent, thus facilitating the study of the plant-endophyte symbiosis in the bioremediation processes.

Introduction

Currently, with the wide application of synthetic dyes, their effluents could cause severe damage to the environment. As one of the most important groups of synthetic dyes, triphenylmethane (TPM) dyes such as cotton blue (CB), crystal violet (CV), malachite green (MG) and methyl violet (MV) in textile, leather, cosmetic, pharmaceutical and paper industries poses a direct threat to the environment due to the toxic and carcinogenicity of their degradation products (Daneshvar et al., 2007; Chaudhry et al. 2014; Barapatre et al. 2017; Przystas et al. 2018). As a consequence, effective removal of hazardous TPM dyes from the aqueous solutions as well as detoxification is crucial. Over the past decade, bioremediation are considered an excellent alternative, since the removal processes occurs by a green technology of low-cost and eco-friendly compared with traditional physico-chemical technique (Kaushik and Malik 2009; Ali 2010; Turhan et al., 2012). Previously, it has been reported that there are many microorganisms capable of degrading chromophores of TPM dyes, such as bacteria and fungi (Yang et al. 2009; Chen et al. 2010; Parshetti et al. 2011; Marcharchand and Ting 2017; Roy et al. 2018). Compared with bacteria, the application of fungal biomass in dye wastewater treatment technology has attracted more and more attention (Shedbalkar et al. 2008; Kaushik and Malik 2009).

Generally speaking, fungi remove dyes may take place in two mechanisms either biosorption and/or biodegradation, depending on whether live or dead cells are used (Ali 2010; Marcharchand and Ting 2017; Chen et al. 2019). Biosorption occurs in both live and dead cells, while biodegradation take place only live cells, which latter is a more complete degradation mechanism. In most cases, fungi are capable of degradation of dyes, it has been primarily attributed to their produce the nonspecific lignin-degrading systems, such as manganese peroxidase (MnP), lignin peroxidase (LiP) and laccase (Lac) (Zhuo et al. 2011; Barapatre et al. 2017; Wang et al. 2017). Meanwhile, this has been proven by most widely fungi, for example white-rot fungi *Phanerochaete chrysosporium* (Bumpus and Brock 1988), *Trametes versicolor* (Casas et al. 2009), *Irpex lacteus* (Yang et al. 2016), *Coriolopsis* sp. (Chen and Ting 2015b), *Pleurotus ostreatus* (Morales-Alvarez et al. 2018) and others fungi, such as *Aspergillus* sp. (Kumar et al. 2011; Ali et al. 2016), *Trichoderma asperellum* (Marcharchand and Ting 2017), *Penicillium simplicissimum*, which above mentioned fungal species capable effective decolorization TPM dyes due to their produce at least one of these essential lignin enzymes (Casas et al. 2009; Ottoni et al. 2013; Wang et al. 2017; Ortiz-Monsalve et al. 2019).

It should be noted that even though many studies using fungal decolorization have been reported, exploring new fungal sources is still important due to the diversity of the dye and complexity of the environment (Yang et al. 2009; Sodaneath et al. 2017). To the best of our knowledge, many previous studies have focused on using fungi to decolourise synthetic dyes (such as azo, anthraquinone and triphenylmethane) especially white-rot fungi, which were from dye-contaminated environments such as sewage, soils (Yang et al. 2009; Almeida and Corso 2018). However, the use of endophytic isolates for the decolourisation TPM dyes less to be explored. In terms of endophytic fungi, which as a hot research topic nowadays in pharmaceuticals, agriculture and industry owing to their robust morphology and diverse ecosystem amenities (Zheng et al. 2016). Simultaneously, endophytic fungi can metabolize organic contaminants and assist in plant growth, thus facilitating the phytoremediation of polluted environments (Shang et al. 2019). In general, strains isolated from contaminated areas have been reported to have a strong tolerance and potential for remediation to contaminants. Hence, we can seek potential endophytic fungi from extreme environments (as metal-contaminated) for bioremediation of soil, water etc. Based on the above reasons, the aim of this work was to study the potential use endophytic fungi, which was isolated from the metal-contaminated plant, *Sinosenecio oldhamianus*, as a biological agent to remove TPM dyes. The ability to decolor TPM dyes by endophytic isolate under non-nutritive conditions was evaluated. Studying the effect of decolorization conditions (fungal biomass, initial dye concentration, shaking and static), the UV–vis absorption spectra analysis, fourier transform infrared (FTIR) analysis, enzyme activities and phytotoxicity. This work may facilitate a better understanding of the role of endophytic fungi in the phytoremediation of TPM dyes.

Material And Methods

2.1 Endophytic Fungi and Media

The endophytic fungi used in this study were isolated from the roots of *Sinosenecio oldhamianus*. Plant samples were collected from the surrounding areas of factory at Shapingba (106.46°E, 29.65°N) of Chongqing city of China. The endophytic isolations were obtained using the methods described by

Huang et al. (2015). For propagation of the fungal culture potato-dextrose (PD) medium was used. The isolated endophytes were grown onto Mineral basal medium (MBM) agar plates and preliminary screened for their ability to decolourise four types of TPM dyes (CV, MV, MG and CB). The MBM contained (g/L): $FeSO_4 \cdot 7H_2O$, 0.01; $ZnSO_4 \cdot 7H_2O$, 0.01; $MgSO_4 \cdot 7H_2O$, 0.5; $CuSO_4 \cdot 5H_2O$, 0.05; KCl, 0.5; K_2HPO_4, 1; $NaNO_3$, 3; starch, 10; and agar, 18.

2.2 Screening of decolorized strains

The isolated endophytes were grown onto MBM agar plates and preliminary screened for their ability to decolourise TPM dyes. Each TPM dye was added into the agar from a stock solution to a final concentration of 100mg L^{-1}. The agar plates were inoculated with a $5mm^2$ agar plug from a 7-day old fungal culture and incubated in 28°C for a period of 14 days. The colonies which formed an obvious decolorization zone were isolated. The colonies continued to be inoculated on the MBM medium plates containing TPM dye (200mg L^{-1}) and finally a fungus which showed a maximum decolorization zone was obtained. Un-inoculated plates with the respective dyes were used as the control. Each isolate was prepared in triplicate.

2.3 Strain identification

The fungal isolate with the highest decolourise potential against TPM dyes, was taxonomically identified based on its morphological characteristic and also by comparison of the ITS sequences as described in Qin et al. (2018). Briefly, the morphological appearances of the selected fungal isolate were characterized based on mycelium colours, growth patterns, and morphology of vegetative spores' structures. For molecular identification, genomic DNA was extracted 1g chilled mycelia in liquid nitrogen using the CTAB method (Zhang et al. 2006). Extracted fungal DNA was then PCR-amplified using universal primer ITS1 and ITS4 under the following condition: an initial denaturing step at 94°C for 3min, followed by 32 amplification cycles at 94°C for 30s, 56°C for 30s, 72°C for 90s, and a final extension at 72°C for 10min. PCR products were then purified and sequenced. The fungi were classified by comparing the ITS sequences of fungi with the data available in NCBI using BLAST search (http://www. ncbi.nlm.nih.gov/). The resulting sequences were aligned with the Clustal X software (Larkin et al. 2007), with gaps treated as missing data. Phylogenetic tree was built by the neighbor-joining method using Mega 6.0 software. The bootstrap was 1000 replications to assess the reliability of the inferred tree (Tamura et al. 2011).

2.4 Dye decolorization batch experiments under non-nutritive conditions

Fungal biomass was first established by inoculating 100 ml Potato Dextrose Broth (PDB) with three mycelium plugs (0.8cm in diameter) to generate sufficient biomass used for dye decolorization experiments. The inoculated PDB was then incubated as a standing culture (28 ± 2°C) for 5-7days, and the biomass subsequently filtered through a sterile filter paper, then fresh biomass was harvested and washed with sterile distilled water. Each TPM dye (CV, MV, MG, and CB) was weighed and dissolved in 100ml autoclaved distilled water to produce dye solutions. To analyze the effects of different conditions on the efficiency of TPM dyes decolorization, batch experiments were conducted at different fungal biomass inoculum size (1-8g), initial dyes concentrations (50-250mg L^{-1}), static (0rpm) and shaking (150rpm) conditions using decolorization percentage as the index. Untreated (non-inoculated) dye solutions were designed as controls. The samples were centrifuged at 5000rpm for 10min. The supernatants were measured by monitoring the absorbance of each dye in the culture medium at its respective maximum absorption wavelength (590nm for CV, 585nm for MV, 617nm for MG and 599nm for CB) using a UV-Vis spectrophotometer (Libra S12, Biochrom). The dye removal potential was expressed as decolorization efficiency (DE, %) as follows :

DE（）=

- Analysis of decolorizing mechanism

2.5.1 Analysis of biomass absorption and enzymolysis contributions on the decolorization of TPM dyes

TPM dyes solution (50mg L^{-1}) was mixed with fungal biomass (4g) under shaking (150rpm) conditions at 30°C for 7 day, to calculate the decolorization rate as in Section 2.4. Control experiments with the dead biomass which were sterilized at 121 °C for 30 min also be carried out (Ting et al. 2016; Wang et al. 2017).

2.5.2 UV-vis spectra of dye solution

UV-vis spectral analysis was performed to determine the possible occurrence of dyes removal with fungal strains treatment, by comparing the change in peaks of dye samples at initial stage of experiment and post-treatment (from section 2.5.1). Absorption peaks for each TPM dye were detected by means of UV-vis (TECAN®, Infinite M 200 plate reader) at wavelengths 400−800nm. Spectra peaks were plotted and compared (Kalpana et al. 2012).

2.5.3 Fourier transform infrared of fungal

FTIR analysis was performed to characterize the functional groups present on the cell wall of live cells and dead cells of fungal biomass. To confirm the existence and responsibility of functional groups on the fungal biomass in biosorption, ftir spectra of the biomass samples (from section 2.5.1) before and after biosorption were obtained using FT-IR Spectrum (Perkin Elmer, USA) conducted in ambient temperature. Data were collected within the mid-infrared region from 4000 to 400cm^{-1} (20-scan speed) (Chew and Ting 2016; Munck et al. 2018).

2.6 Enzyme assays

Enzyme activities were estimated spectrophotometrically by using the the optimized crude supernatant fractions. The control was prepared by inoculating PDB with 5 mycelium plugs (5mm^2) and incubated with agitation (150 rpm, 30 ± 2°C). Enzyme activity was measured after 24h in the treatment and control groups. MnP activity was determined by oxidation of $MnSO_4$ (Asgher et al. 2016). The reaction mixture had a final volume of 2ml containing 0.05M of $MnSO_4$ in 0.1M sodium acetate buffer pH 5 and supernatant (enzyme sample). The reaction was initiated by addition hydrogen peroxide at a final concentration of 0.5mM. The mixture was incubated for 10min at 25°C and the increase in absorbance was measured at 470 nm. The LiP activity was measured by the oxidation of veratryl alcohol to veratryl aldehyde. The final 3.0ml of reaction volume contained 0.2M tartaric acid, 10mM veratryl alcohol, 2M H_2O_2 and supernatant (enzyme sample). Controls were maintained without addition of H_2O_2. The samples were incubated at 25°C for 15min and increase in absorbance was monitored spectrophotometrically at 310nm (Takamiya et al. 2008). The Lac assay was performed by detecting oxidation of 2, 2'- azinobis (3-ethylbenzthiazoline)-6-sulfonate (ABTS) in control and treated samples via colorimetric change at 420nm (Chen and Ting 2015a, b). The reaction mixture contained 5mM ABTS in 0.1M sodium acetate buffer (pH 5.0) and supernatant (enzyme sample). One enzyme unit was defined as the amount of enzyme required catalyzing the conversion of 1 micromole of substrate per min at 25°C.

2.7 Phytotoxicity studies

Toxicity of TPM dyes before and after treatment was inspected against two commonly cultivated crops, which are *Vigna* radiata and *Zea mays* plant seeds. About 5mL each of 100mg L^{-1} TPM dyes solution with and without fungal treatment (biomass 2g, 150 rpm, 30 ± 2°C) was used for the assay. Ten seeds of each plant were sowed in the petri plates and with sterile distilled water as a control at 28°C culture for 5 days (Kalpana et al. 2012). The phytotoxicity was evaluated on the base of their percentage Germination (%) and the shoot length (plumule) and root length (radicle) measured after the incubation for 5 days.

2.8 Statistical Analysis

All data in this paper are the mean value (±SD) of three independent replicates. SPSS 19.0 software was used for statistical analysis. Statistically significant differences among the experimental treatments were analyzed using one-way analysis of variance (ANOVA) followed by Duncan's test at 0.05 probability level.

Results And Discussion

3.1 Screening of TPM dyes decolorization strain

A total of 14 strains of endophytic fungi were isolated from the roots of *Sinosenecio oldhamianus* samples collected from the surrounding areas of factory at shapingba (106.46°E, 29.65°N) of Chongqing city of China. The decolorization capability of these fungal strains was assessed on MBM plates with 4 types of TPM dyes (CV, MV, MG and CB) inoculated at 28°C for 2 week. As shown in Supplementary Table 1 the tested fungal strains on solid medium exhibited a different potential of TPM dyes decolourisation after 14-day cultivation. Among, four strains (SWUSI4, SWUSI6, SWUSI9 and SWUSI13) that caused all tested four TPM dye decolorization were screened out at dyes concentrations 200mg L^{-1} (Fig. 1). The dye decolorization results on agar plates showed that these fungal strains had the ability to decompose all tested four TPM dyes. This result conforms to most observations (Jasinska et al. 2012; Yang et al. 2016), suggesting that different fungi had different dye decolorization abilities, even those that belonged to the same dye. Simultaneously, the effectiveness of fungi decolorization is related to the adaptability and activity of the selected strains. Obviously, strain SWUSI4 had the capability to completely decolorize all four different TPM dyes in the study of solid decolorization (Fig. 1, Supplementary Table 1). Moreover, compared with others three isolate SWUSI6, SWUSI9 and SWUSI13, the decolorization effect of isolated strain SWUSI4 was the best. Hence, isolate SWUSI4 was selected for further taxonomical identification as well as more detailed decolorization study.

3.2 Identification of isolate SWUSI4

Morphologically, isolate SWUSI4 produces white fast-growing colonies with a diameter of 8.34cm (±0.26) after 5 days of growth on PDA at a temperature of 28°C, aerial mycelium abundant, woolly, at first white but later becoming yellowish, reverse white (Supplementary Fig. S1A, B). Advancing hyphae dichotomously branched, 4.54μm (±1.76) diameter; and air-borne hyphae dividing into one-celled arthroconidia which remain cylindrical or become ellipsoidal or slightly barrel-shaped, 4.08 (±0.81) × 6.20 (±2.16) μm (Supplementary Fig. S1C), which is consistent with the morphological description of *Bjerkandera adusta* R59 in the published literature (Kornillowicz-Kowalska et al. 2006). For isolated SWUSI4, the 5.8SrDNA gene sequence was determined and classified in the genus *Bjerkandera* sp. on the basis neighbor-joining analysis compared to other similar fungi stains (Fig. 2). This identity was provided on the basis of the nucleotide sequence having a 99% homology (E value of 0.0; 99% query coverage) with that of *Bjerkandera adusta* strain MJ01 deposited in GenBank (accession number HQ327995.1) and *Bjerkandera adusta strai*n SM27 deposited in GenBank (accession number KU055647.1). Based on molecular taxonomy investigation of the strain SWUSI4, this fungus was identified as *Bjerkandera adusta*. And the nucleotides sequences were submitted to GenBank and provided a GenBank accession number **MN640911**.

3.3 Dye decolorization activities of different conditions by *adusta* SWUSI4

3.3.1 Effects of biomass on dye removal

Biomass dosage also played a major role in the decolorization process. The effect of biomass dosage was evaluated at the concentration of 100mg L^{-1} (100mL) at 30°C for 14day. As revealed in Fig. 3A, our result showed that application of 4g of biomass was sufficient to achieve the decolorization

efficiency (DE %) for CV (85%) and MG (95%), while CB and MV required 6g to achieve maximum DE 89% and 92%, respectively. When the biomass dosage was 6g, decolorization rate reached 89 and 97% for CV and MG, respectively. In terms of CV and MG, the maximum DE was observed when the biomass dosage was 6g, but there were no conspicuous differences between biomass dosage of 6g and 4g (Fig. 3A). The benefit of using more biomass has also been reported in other studies Kaushik and Malik et al. (2009); Wang et al. (2017); Bankole et al. (2018); Almeida and Corso (2018). The increase in dye sorption relative to adsorbent dose is attributed to an upsurge in the fungal surface area, which leads to more binding sites for dye molecules and provides more substances responsible for biodegradation such as enzymes. In general, decolorization efficiency rose with the increase of biomass dosage. However, our results showed that the percentage of decolorization for all tested four TPM dyes increased with increasing biomass dosage but declined at much higher biomass dosage. For example, when biomass ranged from 6 to 8g, DE value was significantly down to 84%~74% (CV), 92%~83% (MV), 96%~82% (MG) and 89%~77% (CB) respectively, (Fig. 3A). This results showed that the use of higher biomass (6 or 8g) did not further enhance or improve decolorization efficiency due to the use of biomass dosage may was limited by the dye initial concentration in the culture medium and not by the dosage of inoculum (Chen et al. 2015a, b). Thus, in this case, less biomass was considered to remove low concentration of TPM dyes, vice versa. To summarize, the results obtained from this investigation demonstrated that suitable biomass could be efficiently employed as a low-cost and eco-friendly biosorbent for TPM dye removal.

3.3.2 Influence of initial dye concentrations on decolorization

Effect of initial dye concentration on the decolorization ability of *Bjerkandera adusta* SWUSI4 was studied by adding the fungal biomass (2g) to CV, MV, MG and CB solution (100mL) with different initial concentrations (50, 100, 150, 200 and 250mg L^{-1}, respectively). Decolorization efficiency was calculated after 14 day at 30°C. For four tested dyes, it was evident that the DE declined when initial dye concentration increased. At the dye concentration of 50mg L^{-1}, *Bjerkandera adusta* SWUSI4 allowed 85, 90, 94 and 80% DE of CV, MV, MG and CB, respectively (Fig. 3B). Additionally, when the initial dye concentration was 100mg L^{-1}, DE reached 72, 81, 90 and 70% for CV, MV, MG and CB, respectively. However, our result showed that the decolorization efficiency between the dye concentration of 50 and 100mg L^{-1} had little difference for four tested TPM dyes (except CV). Whereas, when the initial dye concentration was 250mg L^{-1}, DE reached 34%, 37%, 67% and 35% for CV, MV, MG and CB, respectively (Fig. 3B). Similar results have also been reported by Lin et al. (2010), who found that the decolorization efficiency of *Mucoromycotina* sp. declined with increasing initial dye concentrations. The implications of high initial dye concentrations agreed to most investigations (Chen and Ting 2015a, b; Wang et al. 2017; Almeida and Corso 2018), thus suggesting as the toxicity of dye could be more pronounced at higher dye concentrations which may suppress the microbial growth. In order to improve the decolorization ability, 50mg L^{-1} TPM dyes solution was chosen as the optimum dye concentration.

3.3.3 Effect of shaking and stationary conditions

To determine the effects of static and shaking conditions on decolorization, thus this effect was studied under two different conditions (0rpm and 150rpm, respectively), by treating 100ml of dye solutions with fungal biomass 2.0g, initial dye concentrations 100mg L^{-1} as with other experimental conditions remained constant. Comparatively, SWUSI4 in shaking condition were more effective in decolorizing TPM dyes than static condition (expect MG) (Fig. 3C). Among them, the DE on CV, MV and CB were significantly higher in shaking condition with means 72%, 81% and 70% as compared to 27%, 47% and 58% in static condition, respectively (Fig. 3C). All the T-test comparison for shaking and static conditions of SWUSI4 for CV (t = 19.79, df = 14, sig. two-tailed = 0.000), MV (t = 14, df = 14, sig. two-tailed = 0.000), CB (t = 2.95, df = 14, sig. two-tailed = 0.010) were significantly different. By contrast, the DE of MG dye under shaking condition is similar to static condition (90% vs. 91%) (Fig. 3C). In general, shaking cultures can supply better oxygen transfer and nutrient distribution as compared to the stationary cultures (Kaushik and Malik 2009). Similiar to the decolouration of MG by SWUSI4, another fungus *Coriolopsis* sp. 1c3 has been demonstrated better decolorization activities in the absence of oxygen (Chen and Ting 2015b). Unlike the treatment of MG, the higher decolourization of CV and MV by SWUSI4 under shaking condition than a static condition was observed, which was inconsistent with the findings that *Penicillium simplicissimum* KP713758 decolorize them more efficiently under static conditions with limited oxygen (Chen and Ting 2015a). Besides, it has been reported the shaking condition was better for faster and complete adsorption and decolourization of MV and CV by *Coriolopsis* sp., as well as CB by *Penicillium simplicissimum* KP713758 or *Coriolopsis* sp. as compared to static conditions (Chen and Ting 2015a, b). We assumed that the discrepancy between aerobic and anaerobic decolorization seemed to be related to fungal species. According to the authors, the higher decolourization under shaking condition than a static condition is primarily dependent on the oxidative reactions by key enzymes such as LiP and Mnp (Shedbalkar et al. 2008; Zhuo et al. 2011). In another case, the process of decolorization does not require oxygen and most possibly involved reductive reactions by a different set of reductases. Under aerobic conditions, oxygen and dye molecules compete for the reduced electron acceptor, implicating enzymatic activities, leading to inferior DE (Jadhav and Govindwar 2006; Rauf and Ashraff 2012). Thus, the static and shaking incubation conditions have different impacts on the efficiency of the decolourization process may be because the relative contribution of each enzyme to dye decolorization is different for each fungal strain. All in all, our results demonstrated that shaking incubation conditions could be efficiently decolorization.

Analysis of decolorizing mechanism

3.4.1 Biomass absorption or adsorption and enzymolysis contributions of *B. adusta* on the removal of TPM dyes

It is known that decolorization occurs first through fungal mycelium adsorption, followed by degradation (Parshetti et al. 2011). However, to the best of our knowledge adsorption are typically of the same importance and effect for decolorization mediated by dead cells and live cells, once the mycelia were dead, the decolorization only depended on the absorption (Wang et al. 2017). As shown in Fig. 4, TPM dyes solution (50mg L^{-1}) was mixed with fungal biomass (4g) under shaking (150rpm) conditions at 30°C for 7day, the decolorization efficiency of live cells for MG, MV, CB and CV were 97%, 94%, 94% and 92%, respectively. By contrast, dead cells showed decolorization capacities of 72%, 71%, 64% and 53% for MG, MV, CB and CV, respectively. All the T-

test comparison for live cells and dead cells of SWUSI4 for MG (t = 26.42, df = 14, sig. two-tailed = 0.000), MV (t = 15.00, df = 14, sig. two-tailed = 0.000), CB (t = 18.88, df = 14, sig. two-tailed = 0.000) and CV (t = 30.05, df=14, sig. two-tailed=0.000) were significantly different (Fig. 4). Furthermore, the decolorization process by live cells of *Bjerkandera adusta* SWUSI4 was rapid compared to dead cells. Live cells achieved DE for CV, MV, MG and CB allowed rapid decolorization within 24h (91%, 94%, 96% and 93%, respectively). By contrast, dead cells achieved DE for CV, MV, MG and CB allowed 45%, 63%, 68% and 55%, respectively, decolorization within 24h (Fig. 5). In generally, the higher DE by live cells as opposed to dead cells has been reported in other studies as well Ting et al. (2016); Przystas et al. (2018); Chen et al. (2019). This has been primarily attributed to the biodegradation of live cells because they can produce the lignin modifying enzymes, such as MnP, LiP and Lac (Srinivasan and Viraraghavan 2010; Marcharchand and Ting 2017; Munck et al. 2018). On the other hand, according to Casas et al. (2009) described, the occurrence of biosorption can be concluded by the dye-colored fungal cells after decolorization. In our study, after the decolorization the color of dead cells was same as corresponding TPM dyes, respectively, while the color of live cells was observed to be closest to the original mycelium color (data not shown). This indicated that live cells may to degrade dye particles adsorb on the surface of mycelia to a certain extent by lignin modifying enzymes. Thus, absorption presumably played a major role in the decolorization as well as degradation also had a certain role when using live cells.

3.4.2 UV-Vis Analysis

As shown in Fig. 6, for both treatments with live and dead cells of *B. adusta* SWUSI4 for 7days, these absorbance peaks were obviously observed to reduce or disappear after decolorization. According to the reports (Ting et al. 2016; Ortiz-Monsalve et al. 2019; Munck et al. 2018), the disappearance or reduction of peaks in dyes can be attributed to the enzymatic biodegradation or biosorption of biomass. In our results, the complete dissolution of maximum absorption peaks were clearly observed for CB and MG treated with live cells of *B. adusta* (Fig. 6a, c). For CV and MV treated with live cells, the corresponding maximum absorption peak dramatically decreased in intensity after application with SWUSI4 (Fig. 6b, d). For CV, MV, MG and CB treated with dead cells of *B. adusta*, the maximum absorption peaks remained detectable after 7 days (Fig. 6e, f, g and h). Furthermore, the decrease degree of the maximum absorption peaks of four tested TPM dyes seems to be proportional to the decolourization percentage of their corresponding dyes detected, especially from 0 day to 1 day irrespective of whether live or dead cells of *B. adusta* SWUSI4 were used (Fig. 6). Previously, it has been reported that a decrease in absorbance peaks and appearances of a new peak reflects the removal of dye via biodegradation leading to biodecolourisation, while dead cells destroyed the absorption peak via biosorption (Asad et al. 2007; Chen and Ting, 2015). Association with decolorization percentage and UV−vis analysis, it can be stated that the decolorization of four tested TPM dyes carried out by live cells of isolate SWUSI4 were related to both biodegradation and biosorption, while dead cells only via biosorption.

3.4.3 FTIR analyses

It should be noted that the FTIR spectrum of the fungal biomass in both live and dead cells supports the presence of chemical groups, which are the primarily responsible for the binding of dyes molecules. From the major peaks observed, the primary functional groups of untreated live and dead fungal cells included hydroxyl, amino, phosphoryl, carbonyl and nitro groups (Fig. 7). These functional groups, consisting of both positively-charged and negatively-charged groups are important to attract both basic (CV, MV and MG) and acidic (CB) TPM dyes through electrostatic attraction which is the basis of the biosorption mechanism of dye removal.

For live cells, the treatments with CV, MV, MG and CB caused peaks to shift at 3394cm^{-1} (representing O-H and N-H groups), 2368cm^{-1} (C=C stretching of ester), 1654cm^{-1} (C=O stretching and N-H deformation of amide I band), 1076cm^{-1} (denoting C-C, C=C, C-O-C and C-O-P groups of polysaccharides) and 528cm^{-1} (nitro compounds and disulphide groups) (Table 1; Supplementary Fig.S2). Interactions between phosphoryl group and TPM dyes may have occurred according to the shift of a peak at 1076cm^{-1} and disappearance of a peak at 1149cm^{-1}. Furthermore, another peak at 1251cm^{-1} (also denoting the phosphate group) was masked after CV treatment and shifted to 1261cm^{-1} after MG treatment although no changes in this peak was not observed for CB and MV treated live cells. In additional, new peak at 1741cm^{-1} were detected (C=O group) in all dye-treated live cells. On the contrary, the involvement of C-H stretching virations at 2926 and 2339cm^{-1}, and amide III group at 1456cm^{-1} in dye adsorption were not prominent (Table1; Supplementary Fig.S2).

Dye-treated dead cells displayed similar changes in vibrational frequencies as for live cells, though with was more new peaks appearing (Table 2; Supplementary Fig. S2). The peaks at 3415, 2368, 1404 and 1033cm^{-1} shifted after exposure to the four dyes. In addition, a weak shift from 2926 to 2924cm^{-1} (C-H asymmetric stretching) was observed for CV, MV and MG treated dead cells. All four dyes caused the disappearance of two peaks at 1327 and 775cm^{-1}, and the emergence of a new peak at 1741cm^{-1}(C=O stretching of ester). Further, new peak at 2857cm^{-1} were detected (C-H stretching) in CB-treated dead cells, whereas peaks at 927cm^{-1} masked in all-treated dead cells but MG. The MV and MG treatments result in the emergence of a new peak at 1342cm^{-1} (Amide III), and shifting of existing peaks at 1456 and 1404cm^{-1}(C-N stretching) (Table2; SupplementaryFig.S2). Differently, the CV and CB treatments led to the emergence of a new peak at 1344cm^{-1}, at 1456cm^{-1} in dye adsorption were not prominent and an existing peak at 1404 cm^{-1} shifted to1415cm^{-1}.

The changes in vibrational frequencies recorded via FTIR analyses on the chemical surface composition of dye-treated *B. adusta* confirmed the involvement of biosorption in dye removal. Several authors have suggested that the removal of dyes is attributed to the adsorption of functional groups. For example, Yang (2011) showed that the biosorption of Acid Blue 25 by dead (autoclaved) *Penicillium* YW 01 involved amine, amide and carboxyl groups. Another fungi *Aspergillus fumigatus,* removal of Acid Violet 49 by dead (through freezing) was attributed to amino, carboxyl, phosphate, and sulfonyl groups (Chaudhry et al. 2014). Similarly, Chen et al. (2019) also reported that removal of TPM dyes by live cells and dead cells of *Penicillium*

simplicissimum involved amino, hydroxyl, phosphoryl, and nitro groups etc. By contrast, in our study, several common functional groups (hydroxyl, amino, phosphoryl, carbonyl and nitro groups) were detected in both live cells and dead cells to participate in the biosorption of dyes in the FTIR spectrum. Therefore, the involvement of chemical groups of SWUSI4 in the removal of TPM dyes substantiated biosorption as part of the dye removal mechanisms.

3.5 Enzymatic activities

In order to get additional insight into the enzymolysis contributions of SWUSI4 on the removal of dye, the enzyme activities of Lac, MnP and LiP were monitored after 24hours in the treatment and control groups. As shown in Table 3, our results demonstrated that SWUSI4 produced more LiP and MnP as their levels were significantly induced compared to controls in the presence of TPM dyes. Differed from LiP and MnP, Lac activities demonstrated to be significantly lower than in the control. The levels of MnP and Lip were significantly higher in all TPM dyes compared to the level of Lac levels, indicating SWUSI4 may rely more on LiP and MnP oxidase for biodegradation. Additionally, MnP and LiP activity in MG was higher than that in MV, indicating that the relative contribution of each enzyme to dye decolorization is different for SWUSI4.

Generally, the relative contributions of LiP, MnP and Lac to the decolorization of dyes may be different for each fungus (Srinivasan and Viraraghavan 2010; Wang et al. 2017). Previously, *Phanerochaete chrysosporium* have been reported as Lip producers able to decolorize CV (Bumpus and Brock 1988), *Irpex lacteus* as Mnp producers able to decolorize MG (Yang et al. 2016; Duan et al. 2018), *Pleurotus ostreatus* as Lac producers able to decolorize MG and CV (Morales-Álvarez et al. 2018) and *Coriolopsis* sp. as Lip and NADH-DCIP reductase producers able to decolorize CV, MV and CB, MG, respectively (Chen and Ting 2015b). Besides fungi, contribution of these enzymes in biodegradation process highly depends on type of dyes (Al Farraj et al. 2019). For instance, Chen and Ting (2019) revealed that all three enzymes the activities of manganese peroxidase and triphenylmethane reductase were significantly enhanced activities in response to MG, whereas only tyrosinase activities were higher when inoculated into MV and CB. Similarly, *Penicillium simplicissimum* (isolate 10) has been showed as higher levels of LiP and NADH-DCIP reductase were detected in cultures supplemented with MV and CV (Chen and Ting 2015b). Therefore, according to the above mentioned this study was conducted to detect SWUSI4 may have a similar enzymes to degraded TPM dyes. For this reason we studied the enzymes produced by endophytic isolate SWUSI4. As a whole, the strain SWUSI4 showed that the activity of MnP and Lip are higher than Lac in this study. As such, MnP presumably played an important role in the decolorization as well as Lip also had a certain role and therefore can regulate biodegradation of TPM dyes to some extent.

3.6 Phytotoxicity test

Dyes must be detoxifying before they are released into environment as the presence of toxic dyes in waste water can affect the plant growth and development. Generally, plants belong to the group of sensitive indicators of remediation (Parshetti et al., 2010). Phytotoxicity studies on *Vigna radiata* and *Zea mays* demonstrated that dye toxicity of CV, MV, MG and CB were successfully reduced through biosorption and biodegradation of *Bjerkandera adusta* (isolate SWUSI4). The germination rate, shoot and root length of germinated seeds were observed and presented in Table 4. The seeds germination rate in *Vigna radiata* was not affected by CB (100%), but was inhabited by CV, MV and MG (85, 90 and 80%, respectively). Similarly, the inhibition of CV, MV, MG and CB on germination of *Zea mays* were 70, 80, 60 and 90% respectively, compared with sterile distilled water (Table 4). Meanwhile, seed germination of *Vigna radiata* was enhanced and improved by 100% for all tested four TPM dyes compared to untreated dye sample with isolate SWUSI4 treatment. Similarly, seed germination of *Zea mays* was also increased by 93, 95, 90 and 100% for CV, MV, MG and CB of isolate SWUSI4 treatment, respectively. On the other hand, compared to untreated TPM dyes, the enhanced and significant growth of the shoot and root of *Vigna radiata* and *Zea mays* suggests reduced toxicity after treatment ($p < 0.05$) (Table 4). In additional, in terms of dyes, CB (at 100mg L^{-1}) was considered as less toxic than others as untreated CB solutions resulted in seedlings with germination rate, root and shoot length similar to those in control (without dye application), and the shoots were slightly longer. In case of plant, *Vigna radiata* was less affected than *Zea mays*, suggesting that *Zea mays* might have higher sensitivity towards dye toxicity compared to *Vigna radiata*. As a whole, the result suggests that the all four tested TPM dyes were toxic to both plants, while the metabolites formed after treatments were less toxic or nontoxic, which signifies the detoxification of TPM dyes by *Bjerkandera adusta* SWUSI4 (Chen et al. 2019).

Conclusions

This study is the first to report that effectiveness endophytic fungi isolated from the metal-contaminated *Sinosenecio oldhamianus*, was able to decolourise TPM dyes (CV, MV, MG, and CB). Among them, isolated SWUSI4 (*B. adusta*) had the best decolorization ability for four tested TPM dyes. The decolorization efficiency of SWUSI4 was influenced by initial dye concentrations, fungal biomass, static and shaking. The current study has indicated the efficiency of TPM dyes decolorization using endophytic *B. adusta* SWUSI4 mainly through biodegradation and biosorption after the analysis of decolorizing mechanism. Isolate SWUSI4 has better biosorption of TPM dyes attributed major to the predominance of hydroxyl, amino, phosphoryl and alkane etc. groups on the surface of the cell wall of SWUSI4. Biodegradation played an important role in dye decolorization, which resulted in reduced absorbance peaks for dyes, LiP and MnP levels were significantly induced, and degraded products were also found to be less toxicity compared with before degradation. Hence, this work indicated that the biological decolourization and detoxification of TPM dyes by endophytic isolate SWUSI4 in future can potentially useful tool.

Tables

Table 1 Exemplary FTIR band positions (cm-1) of live cells of isolate SWUSI4 before and after treatment with CV, MV, MG and CB.

Untreated live cells	CV loaded cells	MV loaded cells	MG loaded cells	CB loaded cells	Suggested assignment
3394	**3444**	**3439**	**3425**	**3442**	O-H and N-H stretching vibrations
2926	**2924**	**2924**	**2924**	2926	C-H asymmetric stretching
2368	**2378**	**2378**	**2378**	**2380**	C=C stretching of ester
2339	**2341**	**2341**	**2341**	**2341**	C=C stretching of ester
	1741	1741	1741	1741	C=O stretching of ester
1654	**1645**	**1645**	**1645**	**1645**	C=O stretching and N-H deformation (amide I region)
1562	**1560**	**1560**	**1560**	**1560**	N-H bending in amide II and C-N stretching in -CO-NH-
1456	1456	1456	1456	1456	C-N stretching and N-H bending of amide III
1406	**1413**	**1413**	**1415**	**1415**	C-N stretching and N-H bending of amide III
1251		1251	**1261**	1251	Phosphate group
1149					Phosphate group
1076	**1066**	**1068**	**1070**	**1066**	Phosphate group/C-C, C=C, C-O-C, C-O-P of saccharides
1033	**1022**	**1028**			C-C, C=C, C-O-C, C-O-P of saccharides
	636	636	636	636	Aromatic C-H stretching
528	**524**	**543**	**522**	**522**	Nitro compounds and disulfde groups
426	**418**	**418**	**422**	**420**	Nitro compounds and disulfde groups

Table 2 Exemplary FTIR band positions (cm-1) of dead cells of isolate SWUSI4 before and after treatment with CV, MV, MG and CB.

Untreated dead cells	CV loaded cells	MV loaded cells	MG loaded cells	CB loaded cells	Suggested assignment
3415	**3427**	**3423**	**3439**	**3423**	O-H and N-H stretching vibrations
2926	**2924**	2924	**2924**	2922	C-H asymmetric stretching
				2857	C-H asymmetric stretching
2368	**2372**	**2378**	**2378**	**2378**	C=C stretching of ester
2339	2339	**2341**	**2341**	**2341**	C=C stretching of ester
	1741	1743	1741	1741	C=O stretching of ester
1645	1645	1645	1645	1645	C=O stretching and N-H deformation (amide I region)
1560	1560	1560	1560	1560	N-H bending in amide II and C-N stretching in -CO-NH-
1456	1456	**1458**	**1458**	1456	C-N stretching and N-H bending of amide III
1404	**1415**	**1413**	**1413**	**1415**	C-N stretching and N-H bending of amide III
	1344	1342	1342	1344	Amide III
1327					Amide III
1078	**1068**	**1066**	**1070**		Phosphate group/C-C, C=C, C-O-C, C-O-P of saccharides
1033	**1022**	**1022**	**1024**	**1043**	Phosphate group/C-C, C=C, C-O-C, C-O-P of saccharides
927			927		Phosphate (PO4) in polysaccharides
775					Aromatic C-H stretching / N−O stretching of alcohol
428	**420**	**420**	**422**	**422**	Nitro compounds and disulfde groups

Table 3 Activities of laccase (Lac), lignin peroxidase (LiP) and Manganese peroxidase (MnP) assayed from isolate SWUSI4cultures exposed to TPM dyes compared to control (in Potato Dextrose Broth only). Data presented with standard deviation of mean (±SD) are mean of triplicates. Asterisk "*"indicates significant difference in enzymatic levels from those in Potato Dextrose Broth based on T-test (p < 0.05).

Enzyme	Enzymatic activities derived from				
	PDB	CV	MV	MG	CB
Lac[a]	0.1035±0.0012	0.0200±0.0002*	0.0185±0.0029*	0.0235±0.0010*	0.0036±0.0002*
Lip[a]	0.0067±0.0019	0.0144±0.0022	0.0579±0.0403*	0.0815±0.0268*	0.0339±0.0018*
MnP[a]	0.0459±0.0072	0.1527±0.0496*	0.1796±0.0543*	0.2208±0.0106*	0.1875±0.0194*

[a] Units min^{-1} ml^{-1}.

Tab. 4 Results of phytotoxicity tests of TPM dye and its metabolites produced by the fungus SWUSI4 on *Vigna radiate* and *Zea may*

Parameters studied	Control	TPM dyes				Biodegraded products			
	DW	CV	MV	MG	CB	Treated CV	Treated MV	Treated MG	Treated CB
Vigna radiata									
Germination (%)	100	85	90	80	100	100	100	100	100
Root (cm)	4.40±0.26	2.47±0.15**	2.30±0.10**	1.97±0.15**	2.60±0.10**	3.70±0.20*	3.73±0.61*	3.67±0.35*	4.90±0.20*
Shoot (cm)	4.93±0.15	3.27±0.21**	3.33±0.15**	3.23±0.15**	5.00±0.10	4.53±0.25*	4.47±0.06*	4.67±0.12*	7.90±0.20*
Zea mays									
Germination (%)	100	70	80	60	90	93	95	90	100
Root (cm)	4.72±0.16	2.22±0.18**	2.85±0.04**	2.82±0.02**	3.21±0.08**	4.80±0.82*	4.44±0.27*	4.49±0.20*	7.09±0.68*
Shoot (cm)	3.99±0.06	2.84±0.13**	2.54±0.24**	2.64±0.14**	3.29±0.06**	4.14±0.33*	3.34±0.11*	3.49±0.02*	4.03±0.15*

Values of root and shoot lengths are presented as mean of three experiments ± SD
Root and shoot lengths of seeds grown in TPM dyes are significantly different from that of plants grown in sterile distilled water by **P < 0.01, Root and shoot lengths of seeds grown in biodegraded products of TPM dyes are significantly different from that of plants grown in TPM dyes by *P < 0.05.

Abbreviations

TPM	Triphenylmethane	MBM	Mineral basal medium
CV	crystal violet	ITS	internaltranscribedspacers
MV	methyl violet	DNA	DeoxyriboNucleic Acid
MG	malachite green	CTAB	Cetyltrimethylammonium bromide
CB	cotton blue	NCBI	national center for biotechnology information
LiP	lignin peroxidase	ABTS	2, 2'- azinobis (3-ethylbenzthiazoline)-6-sulfonate
MnP	manganese peroxidase	DE	decolorization efficiency
Lac	laccase	FTIR	fourier transform infrared
PD	potato-dextrose	UV-vis	Ultraviolet-visible

Declarations

Ethics approval and consent to participate

Not applicable

Consent for publication

Not applicable

Conflict of interest statement

The authors declare no conflict of interest.

Data Availability Statements

All data generated or analysed during this study are included in this published article (and its supplementary information files).

Funding

Author contribution statement

Conceived and designed the experiments: TCG. Performed the experiments: TCG, DQ, SHZ, YJP and JRX. Analyzed the data: TCG, DQ and YJP. Contributed eagents/ materials/ analysis tools: TCG, YJP, DQ, BHY, HCS. Wrote the paper: TCG

Acknowledgements

References

Al Farraj, Elshikh, D. A., Al Khulaifi, M. S., Hadibarata, M. M., Yuniarto, T., Syafiuddin, A. (2019). Biotransformation and Detoxification of Antraquione Dye Green 3 using halophilic *Hortaea* sp. *International Biodeterioration & Biodegradation 140*:72-77. https://doi.org/10.1016/j.ibiod.2019.03.011

Ali, H. (2010). Biodegradation of Synthetic Dyes—A Review. *Water, Air, & Soil Pollution 213* (1-4):251-273. https://doi.org/10.1007/s11270-010-0382-4

Ali, H. M., Shehata, S. F., Ramadan, K. M. A. (2016). Microbial decolorization and degradation of crystal violet dye by *Aspergillus niger*. *International Journal of Environmental Science and Technology*, *13* (12), 2917–2926. https://doi.org/ 10.1007/s13762-016-1117-x

Almeida, E. J. R., & Corso, C. R. (2018). Decolorization and removal of toxicity of textile azo dyes using fungal biomass pelletized. *International Journal of Environmental Science and Technology 16* (3):1319-1328. https://doi.org/ 10.1007/s13762-018-1728-5

Asad, S., Amoozegar, M. A., Pourbabaee, A. A., Sarbolouki, M. N., Dastgheib, S. M. M. (2007). Decolorization of textile azo dyes by newly isolated *halophilic* and *halotolerant* bacteria. *Bioresource Technology 98* (11):2082-2088. https://doi.org/ 10.1016/j.biortech.2006.08.020

Asgher, M., Ramzan, M., Bilal, M. (2016). Purification and characterization of manganese peroxidases from native and mutant *Trametes versicolor* IBL-04. *Chinese Journal of Catalysis*, *37* (4), 561–570. https://doi.org/ 10.1016/S1872-2067(15)61044-0

Bankole, P. O., Adekunle, A. A., Govindwar, S. P. (2018). Enhanced decolorization and biodegradation of acid red 88 dye by newly isolated fungus, *Achaetomium strumarium*. *Journal of Environmental Chemical Engineering*, *6* (2), 1589–1600. https://doi.org/10.1016/j.jece.2018.01.069

Barapatre, A., Aadil, K. R., Jha, H. (2017). Biodegradation of Malachite Green by the Ligninolytic Fungus *Aspergillus flavus*. *Clean-Soil Air Water*, *45* (4), 1–12. https://doi.org/10.1002/clen.201600045

Bumpus, J. A., & Brock, B. J. (1988). Biodegradation of Crystal Violet by the White Rot Fungus *Phanerochaete-Chrysosporium*. *Applied and Environmental Microbiology*, *54* (5), 1143–1150.

Casas, N., Parella, T., Vicent, T., Caminal, G., Sarra, M. (2009). Metabolites from the biodegradation of triphenylmethane dyes by *Trametes versicolor* or laccase. *Chemosphere*, *75* (10), 1344–1349. https://doi.org/10.1016/j.chemosphere.2009.02.029

Chaudhry, M. T., Zohaib, M., Rauf, N., Tahir, S. S., Parvez, S. (2014). Biosorption characteristics of *Aspergillus fumigatus* for the decolorization of triphenylmethane dye acid violet 49. *Applied Microbiology and Biotechnology*, *98* (7), 3133–3141. https://doi.org/ 10.1007/s00253-013-5306-y

Chen, C. H., Chang, C. F., Liu, S. M. (2010). Partial degradation mechanisms of malachite green and methyl violet B by *Shewanella decolorationis* NTOU1 under anaerobic conditions. *Journal of Hazardous Materials*, *177*, 281–289. https://doi.org/10.1016/j.jhazmat.2009.12.030

Chen, S. H., Chew, Y. L., Ng, S. L., Ting, A. S. Y. (2019). Biodegradation of Triphenylmethane Dyes by Non-white Rot Fungus *Penicillium simplicissimum*: Enzymatic and Toxicity Studies. *International Journal of Environmental Research*, *13* (2), 273–282. https://doi.org/10.1007/s41742-019-00171-2

Chen, S. H., Cheow, Y. L., Ng, S. L., Ting, A. S. Y. (2019). Removal of triphenylmethane dyes in single-dye and dye-metal mixtures by live and dead cells of metal-tolerant *Penicillium simplicissimum*. *Separation Science and Technology*:1-11. https://doi.org/10.1080/01496395.2019.1626422

Chen, S. H., & Ting, Y. (2015a). Biosorption and biodegradation potential of triphenylmethane dyes by newly discovered *Penicillium simplicissimum* isolated from indoor wastewater sample. *International Biodeterioration & Biodegradation*, *103*, 1–7. http://dx.doi.org/10.1016/j.ibiod.2015.04.004

Chen, S. H., Su, A., Ting, Y. (2015b). Biodecolorization and biodegradation potential of recalcitrant triphenylmethane dyes by *Coriolopsis* sp. isolated from compost. *Journal of Environmental Management*, *150*, 274–280. http://dx.doi.org/10.1016/j.jenvman.2014.09.014

Chen, S. H., Cheow, Y. L., Ng, S. L., Ting, A. S. Y. (2019). Mechanisms for metal removal established via electron microscopy and spectroscopy: a case study on metal tolerant fungi *Penicillium simplicissimum*. *Journal of Hazardous Materials 362*:394-402. https://doi.org/10.1016/j.jhazmat.2018.08.077

Chew, S. Y., & Ting, A. S. Y. (2016). Common filamentous *Trichoderma asperellum* for effective removal of triphenylmethane dyes. *Desalination and Water Treatment 57* (29):13534-13539. https://doi.org/10.1080/19443994.2015.1060173

Daneshvar, N., Ayazloo, M., Khataee, A.R., Pourhassan, M. (2007). Biological decolorization of dye solution containing Malachite Green by microalgae *Cosmarium* sp. *Bioresource Technology, 98*, 1176-1182. https://doi.org/10.1016/j.biortech.2006.05.025

Duan, Z., Shen, R., Liu, B., Yao, M., Jia, R. (2018). Comprehensive investigation of a dye-decolorizing peroxidase and a manganese peroxidase from *Irpex lacteus* F17, a lignin-degrading basidiomycete. *AMB Express*, *8*, 1–16. https://doi.org/10.1186/s13568-018-0648-6

Huang, Q., An, H., Song, H., Mao, H., Shen, W., Dong, J. (2015). Diversity and biotransformative potential of endophytic fungi associated with the medicinal plant *Kadsura angustifolia*. *Research in Microbiology 166* (1):45-55. http://dx.doi.org/10.1016/j.resmic.2014.12.004

Jadhav, J. P., & Govindwar, S. P. (2006). Biotransformation of malachite green by *Saccharomyces cerevisiae* MTCC 463. *Yeast*, *23* (4), 315-323. https://doi.org/ 10.1002/yea.1356

Jasinska, A., Rozalska, S., Bernat, P., Paraszkiewicz, K., Dlugonski, J. (2012). Malachite green decolorization by non-basidiomycete filamentous fungi of *Penicillium pinophilum* and *Myrothecium roridum*. *International Biodeterioration & Biodegradation 73*:33-40. http://dx.doi.org/10.1016/j.ibiod.2012.06.025

Kalpana, D., Velmurugan, N., Shim, J. H., Oh, B. T., Senthil, K., Lee, Y. S. (2012). Biodecolorization and biodegradation of reactive Levafix Blue E-RA granulate dye by the white rot fungus *Irpex lacteus*. *Journal of Environmental Management*, *111* (2012), 142–149. http://dx.doi.org/10.1016/j.jenvman.2012.06.041

Kaushik, P., & Malik, A. (2009). Fungal dye decolourization: recent advances and future potential. *Environment International*, *35* (1), 127–141. http://dx.doi.org/10.1016/j.envint.2008.05.010

Kornillowicz-Kowalska, T., Wrzosek, M., Ginalska, G., Iglik, H., Bancerz, R. (2006). Identification and application of a new fungal strain *Bjerkandera adusta* R59 in decolorization of daunomycin wastes. *Enzyme and Microbial Technology 38* (5):583-590. http://dx.doi.org/10.1016/j.enzmictec.2005.10.009

Kumar, C. G., Mongolla, P, Basha, A., Joseph, J., Sarma, V. U. M., Kamal, A. (2011). Decolorization and Biotransformation of Triphenylmethane Dye, Methyl Violet, by *Aspergillus* sp Isolated from Ladakh, India. *Journal of Microbiology and Biotechnolog*, *21* (3), 267–273. http://dx.doi.org/10.4014/jmb.1011.11010

Larkin, M. A., Blackshields, G., Brown, N. P., Chenna, R., McGettigan, P. A., McWilliam, H., et al. (2007). Clustal W and Clustal X version 2.0. *Bioinformatics*, *23*, 2947–2948. http://dx.doi.org/10.1093/bioinformatics/btm404

Lin, Y. H., Chen, L., He, X. B., He, Y. Q., Zhou, X. (2010). Biodegradation of aniline blue dye by a fungus *Mucoromycotina* sp. HS-3. *Microbiology China*, *37* (12), 1727–1733.

Marcharchand, S., & Ting, A. S. Y. (2017). *Trichoderma asperellum* cultured in reduced concentrations of synthetic medium retained dye decolourization efficacy. *Journal of Environmental Management*, *203*, 542–549. http://dx.doi.org/10.1016/j.jenvman.2017.06.068

Morales-Alvarez, E. D., Rivera-Hoyos, C. M., Poveda-Cuevas, S. A., Reyes-Guzman, E. A., Pedroza-Rodriguez, A. M., Reyes-Montano, E. A., Poutou-Pinales, R. A. (2018). Malachite Green and Crystal Violet Decolorization by *Ganoderma lucidum* and *Pleurotus ostreatus* Supernatant and by rGlLCC1 and rPOXA 1B Concentrates: Molecular Docking Analysis. *Applied Biochemistry and Biotechnology 184* (3):794-805. http://dx.doi.org/10.1007/s12010-017-2560-y

Munck, C., Thierry, E., Grassle, S., Chen and A. S. Y. Ting, S. H. (2018). Biofilm formation of filamentous fungi *Coriolopsis* sp. on simple muslin cloth to enhance removal of triphenylmethane dyes. *Journal of Environmental Management 214*:261-266. https://doi.org/10.1016/j.jenvman.2018.03.025

Ottoni, C. A., Santos, C., Kozakiewicz, Z., Lima, N. (2013). White-rot fungi capable of decolourising textile dyes under alkaline conditions. *Folia Microbiol (Praha) 58* (3):187-193. https://doi.org/10.1007/s12223-012-0196-4

Ortiz-Monsalve, Valente, S., Poll, P., Jaramillo-Garcia, E., Pegas Henriques, V., A, J., Gutterres., M. (2019). Biodecolourization and biodetoxification of dye-containing wastewaters from leather dyeing by the native fungal strain *Trametes villosa* SCS-10. *Biochemical Engineering Journal 141*:19-28. https://doi.org/10.1016/j.bej.2018.10.002

Parshetti, G. K., Parshetti, S. G., Telke, A. A., Kalyani, D. C., Doong, R. A., Govindwar, S. P. (2011). Biodegradation of Crystal Violet by *Agrobacterium radiobacter*. *Journal of Environmental Sciences*, *23* (8), 1384−1393. https://doi.org/10.1016/S1001-0742(10)60547-5

Parshetti, G.K., Telke, A.A., Kalyani, D.C., Govindwar, S.P. (2010). Decolorization and detoxification of sulfonated azo dye methyl orange by *Kocuria rosea* MTCC 1532. *Journal of Hazardous Materials, 176*, 503−509. https://doi.org/10.1016/j.jhazmat.2009.11.058.

Przystas, W., Zablocka-Godlewska, E., Grabinska-Sota, E. (2018). Efficiency of decolorization of different dyes using fungal biomass immobilized on different solid supports. *Brazilian journal of microbiology 49* (2):285-295. https://doi.org/10.1016/j.bjm.2017.06.010

Qin, D., Wang, L. Han, M. Wang, J. Song, H. Yan, X. Duan, X. Dong, J. (2018). Effects of an Endophytic Fungus *Umbelopsis dimorpha* on the Secondary Metabolites of Host-Plant *Kadsura angustifolia*. *Front Microbiol 9*:2845. https://doi.org/10.3389/fmicb.2018.02845

Rauf, M. A., & Salman Ashraf, S. (2012). Survey of recent trends in biochemically assisted degradation of dyes. *Chemical Engineering Journal 209*:520-530. https://doi.org/ 10.1016/j.cej.2012.08.015

Roy, D. C., Biswas, S. K., Saha, A. K., Sikdar, B., Rahman, M., Roy, A. K., Prodhan, Z. H., Tang, S. S. (2018). Biodegradation of Crystal Violet dye by bacteria isolated from textile industry effluents. *Peerj*, *6*. https://doi.org/10.7717/peerj.5015

Shang, N. J., Ding, M. J., Dai, M. X., Si, H. L., Li, S. G., Zhao, G. Y. (2019). Biodegradation of malachite green by an endophytic bacterium *Klebsiella aerogenes* S27 involving a novel oxidoreductase. *Applied Microbiology and Biotechnology 103* (5):2141-2153. https://doi.org/10.1007/s00253-018-09583-0

Shedbalkar, U., Dhanve, R., Jadhav, J. (2008). Biodegradation of triphenylmethane dye cotton blue by *Penicillium ochrochloron* MTCC 517. *Journal of Hazardous Materials*, *157* (2-3), 472−479. https://doi.org/10.1016/j.jhazmat.2008.01.023

Sodaneath, H., Lee, J. I., Yang, S. O., Jung, H., Ryu, H. W., Cho, K. S. (2017). Decolorization of textile dyes in an air-lift bioreactor inoculated with *Bjerkandera adusta* OBR105. *Journal of Environmental Science and Health Part A-Toxic/Hazardous Substances & Environmental Engineering*, *52* (11), 1099−1111. https://doi.org/10.1080/10934529.2017.1340753

Srinivasan, A., & Viraraghavan, T. (2010). Decolorization of dye wastewaters by biosorbents: A review. J*ournal of Environmental Management 91* (10):1915-1929. https://doi.org/10.1016/j.jenvman.2010.05.003

Takamiya, M., Magan, N., Warner, P. J. (2008). Impact assessment of bisphenol A on lignin-modifying enzymes by basidiomycete *Trametes versicolor*. *Journal of Hazardous Materials*, *154* (1-3), 33−37. https://doi.org/10.1016/j.jhazmat.2007.09.098

Tamura, K., Peterson, D., Peterson, N., Stecher, G., Nei, M., Kumar, S. (2011). MEGA5: Molecular evolutionary genetics analysis using maximum likelihood, evolutionary distance, and maximum parsimony methods. *Molecular Biology and Evolution*, *8*, 2731−2739. https://doi.org/10.1093/molbev/msr121

Ting, A. S. Y., Lee, M. V. J., Chow, Y. Y., Cheong, S. L. (2016). Novel Exploration of Endophytic *Diaporthe* sp. for the Biosorption and Biodegradation of Triphenylmethane Dyes. *Water Air and Soil Pollution*, *227* (109), 1−8. https://doi.org/10.1007/s11270-016-2810-6

Turhan, K., Durukan, I., Ozturkcan, S.A., Turgut, Z. (2012). Decolorization of textile basic dye in aqueous solution by ozone. *Dyes Pigments 92* (3), 897-901. https://doi.org/10.1016/j.dyepig.2011.07.012

Wang, N., Chu, Y., Wu, F. A., Zhao, Z., Xu, X. (2017). Decolorization and degradation of Congo red by a newly isolated white rot fungus, *Ceriporia lacerata*, from decayed mulberry branches. *International Biodeterioration & Biodegradation*, *117*, 236−244. http://dx.doi.org/10.1016/j.ibiod.2016.12.015

Yang, X. Q., Zhao, X. X., Liu, C. Zheng, Y., Y., Qian, S. J. (2009). Decolorization of azo, triphenylmethane and anthraquinone dyes by a newly isolated *Trametes* sp. SQ01 and its laccase. *Process Biochemistry*, *44* (10), 1185−1189. https://doi.org/10.1016/j.procbio.2009.06.015

Yang, X., Zheng, J., Lu, Y., Jia, R. (2016). Degradation and detoxification of the triphenylmethane dye malachite green catalyzed by crude manganese peroxidase from *Irpex lacteus* F17. *Environmental Science and Pollution Research*, *23* (10), 9585−9597. http://dx.doi.org/10.1007/s11356-016-6164-9

Yang, Y., Jim, D., Wang, G., Liu, D., Jia, X., Zhao, Y. (2011). Biosorption of Acid Blue 25 by Unmodified and CPC-modified Biomass of *Penicillium* YW01: Kinetic Study, Equilibrium Isotherm and FTIR Analysis. Colloids Surf. *Biointerfaces*. 88, 521−526. http://dx.doi.org/ 10.1016/j.colsurfb.2011.07.047.

Zhang, D., Yang, Y., Castlebury, L. A., Cerniglia, C. E. (2006). A method for the large scale isolation of high transformation efficiency fungal genomic DNA. *FEMS Microbiology Letters*, *145*, 261−265. https://doi.org/10.1111/j.1574-6968.1996.tb08587.x

Zheng, Y. K., Qiao, X. G., Miao, C. P., Liu, K., Chen, Y. W., Xu, L. H., Zhao, L. X. (2016). Diversity, distribution and biotechnological potential of endophytic fungi. *Annals of Microbiology 66* (2):529-542. https://doi.org/10.1007/s13213-015-1153-7

Zhuo, R., Ma, L., Fan, F., Gong, Y., Wan, X., Jiang, M., Zhang, X., Yang, Y. (2011). Decolorization of different dyes by a newly isolated white-rot fungi strain *Ganoderma* sp. En3 and cloning and functional analysis of its laccase gene. *Journal of Hazardous Materials*, *192* (2), 855–873. http://dx.doi.org/10.1016/j.jhazmat.2011.05.106
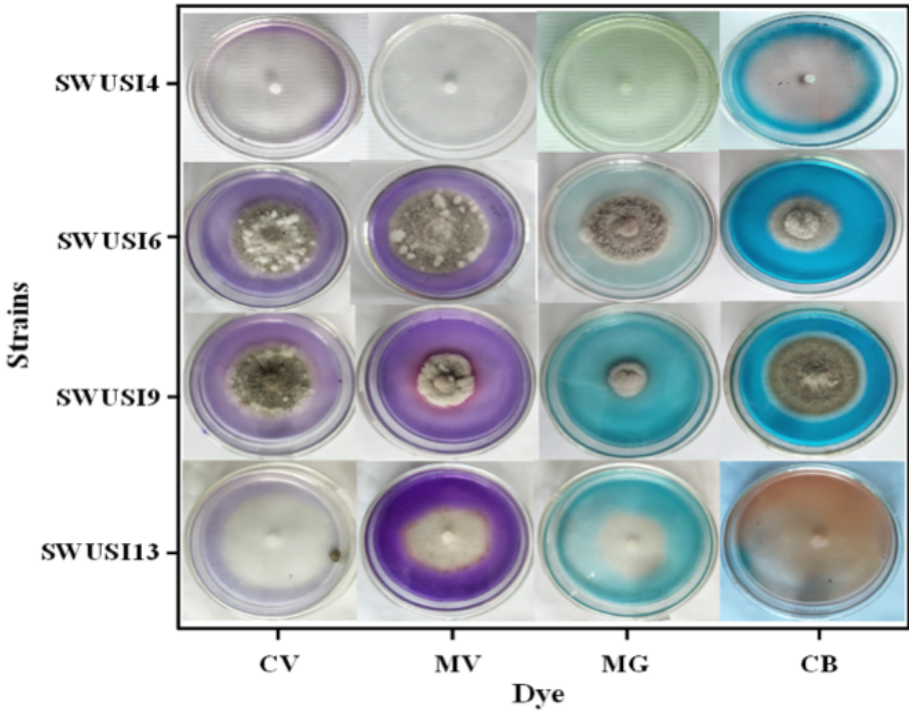
Figures

Figure 1

Dye decolourisation by isolate SWUSI4, SWUSI6, SWUSI9 and SWUSI13 on agar plate medium containing CV, MV, MG and CB after 14 days.
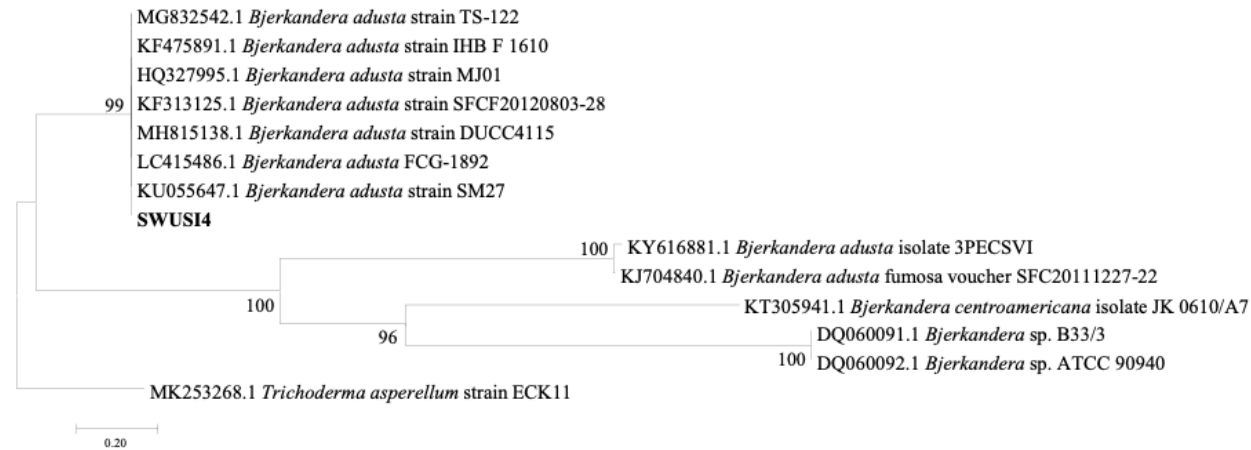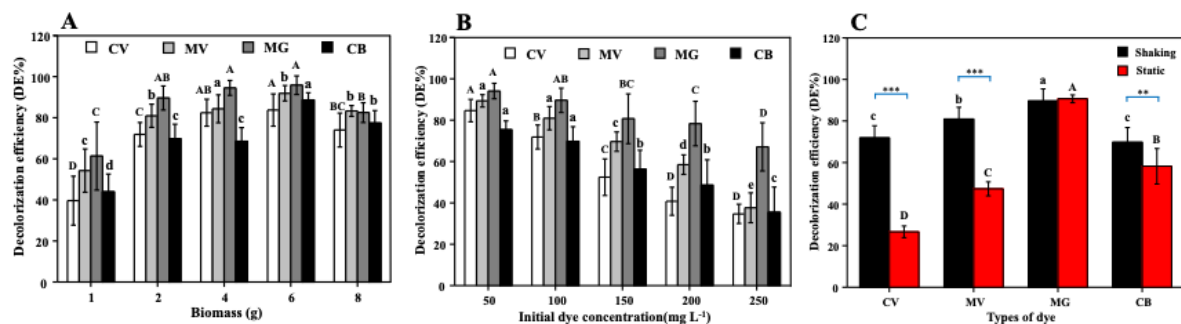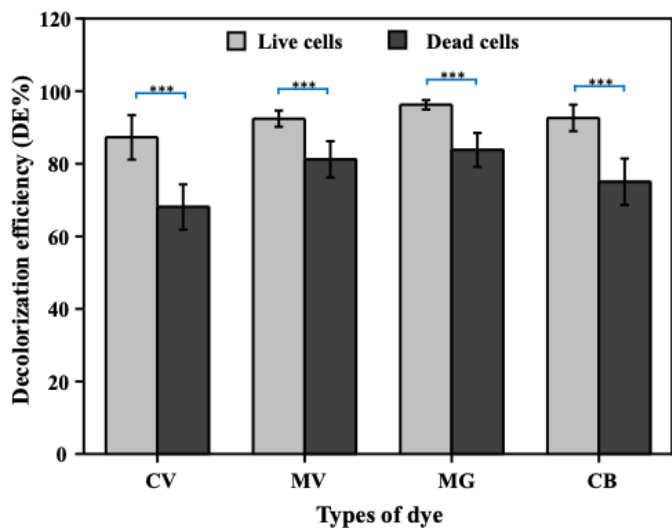

Figure 2

Neighbor-joining tree based on ITS rDNA sequence of the fungus SWUSI4 and its closest ITS rDNA matches in the GenBank.

Figure 3

Optimum decolorization conditions for isolate SWUSI4 A: Influence of biomass (1, 2, 4, 6 and 8 g, respectively) of SWUSI4 on the decolorization activities of CV, MV, MG and CB. B: Influence of initial dye concentrations (50, 100, 150, 200 and 250 mg L-1, respectively) of SWUSI4 on the decolorization activities of CV, MV, MG and CB. C: Influence of static and shaking conditions of SWUSI4 on the decolorization activities of CV, MV, MG and CB. Note: Means with the same letters and captions are not significantly different at Honestly Significant Difference (HSD (0.05)). Mean comparisons are made for means with the same fonts. For example, means designated "A" compared to another mean with "A" Duncan grouping is not significantly different, while "A" compared to "B" and "C" is significantly different. Similarly, means with "a" is not significantly different compared to "a" but is for "b" and "c". "**" indicates significant difference based on T-test ("**" $p < 0.01$, "***" $p < 0.001$). Bars indicate standard deviation of mean (±SD)

Figure 4

4 Influence of live cells and dead cells on decolorization of CV, MV, MG and CB by SWUSI4 at 30 ± 2°C. "***" indicates significant difference based on paired T-test ($p < 0.01$). Bars indicate standard deviation of mean (±SD)
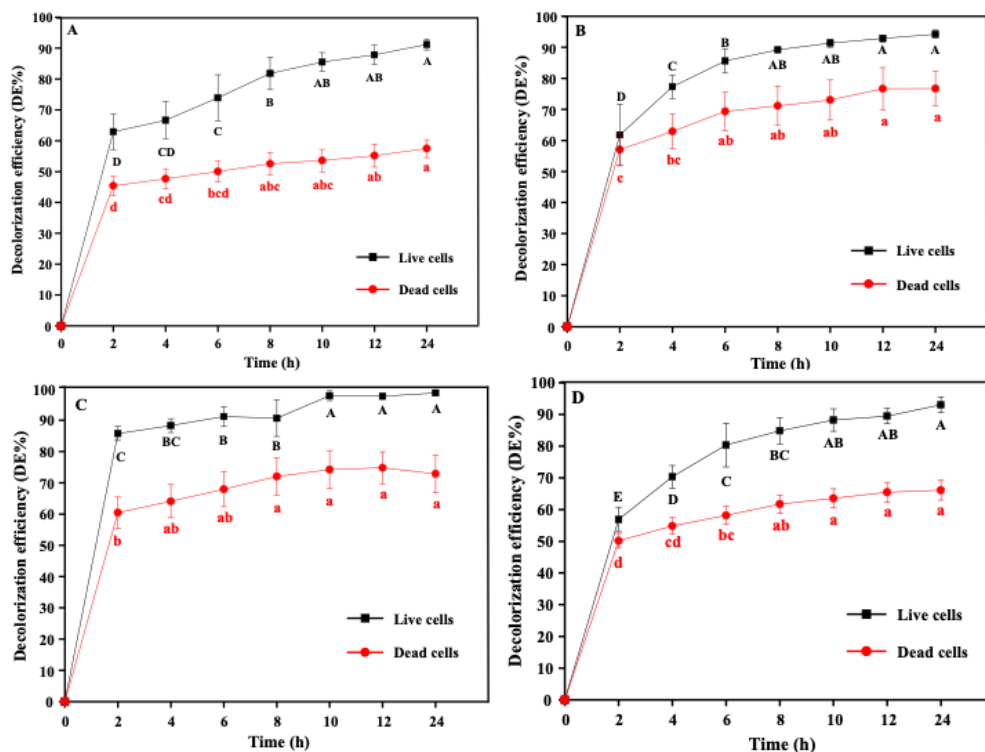
Figure 5

Decolorization efficiency (DE%) of live and dead cells of SWUSI4 on A crystal violet (CV), B methyl violet (MV), C malachite green (MG) and D cotton blue (CB) throughout the 24h experimental period after the optimization.
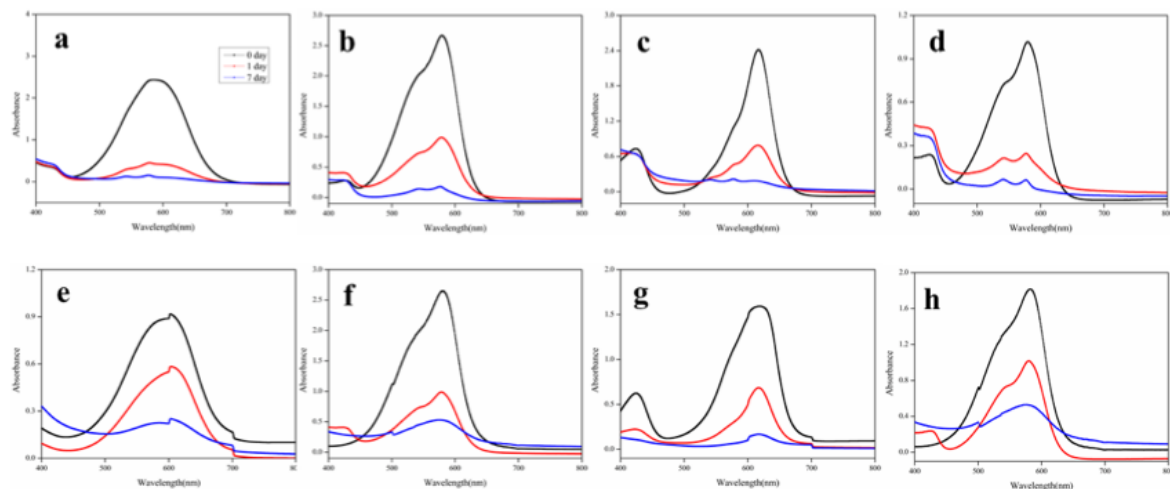

Figure 6

The UV-vis spectrum analysis derived from a-CB + live cells, b-CV + live cells, c-MG + live cells, d-MV + live cells, e- CB + dead cells, f- CV + dead cells, g-MG + dead cells, h-MV + dead cells. Analysis was conducted at the start of the experiment (day 0) and at day 1, day 7 post-treatment, respectively.

Figure 7

FTIR spectra of biomass of Bjerkandera adusta SWUSI4 (a) Un-treatment live and dead cells,

Supplementary Files

This is a list of supplementary files associated with this preprint. Click to download.

- supplement1.docx